Hindawi
Mathematical Problems in Engineering
Volume 2020, Article ID 9862158, 20 pages
https://doi.org/10.1155/2020/9862158

Research Article

On the Dimensional Consistency Aware Fractional Domain Generalization of Simplest Chaotic Circuits

Rawid Banchuin

Faculty of Engineering and Graduated School of Information Technology, Siam University, Bangkok, Thailand

Correspondence should be addressed to Rawid Banchuin; rawid_b@yahoo.com

Received 14 December 2019; Revised 5 February 2020; Accepted 12 February 2020; Published 19 March 2020

Guest Editor: Jesus M. Muñoz-Pacheco

In this research, we generalize the simplest Chua's chaotic circuit which is even more simpler than the four-element Chua's circuit in terms of number of elements and the novel simplest chaotic circuit in the fractional domain by using the fractional circuit elements. Unlike the previous works, the time dimensional consistency aware generalization has been performed for the first time in this work. The dynamics of the generalized fractional nonlinear circuits have been analyzed by means of the fractional calculus based on the modified Riemann–Liouville fractional derivative where the Lyapunov exponents and dimensions have also been numerically calculated. We have found that including the dimensional consistency significantly alters the dynamic of the obtained fractional domain Chua's circuit from that of the previous dimensional consistency ignored counterpart as different Lyapunov exponents and dimensions can be obtained. The conditions for both fractional domain circuits which cease to be chaotic have also been determined where such condition of Chua's circuit presented in this study is different from that of the previous work. This is because the time dimensionalconsistency has been included. The dynamical analyses of these circuits have also been performed where their conditions for being nonchaotic have been verified. Moreover, their emulators have also been realized.

1. Introduction

The fractional calculus and its related differential equation, i.e., FDE, which are the extensions of the conventional integer calculus and the ordinary differential equation (ODE), have been extensively utilized in various research areas, e.g., signal processing, biomedical engineering, electronics, robotics, and control theory [1–11]. The FDE has been used in the fractional domain analysis of electrical circuits in which their orders are fractional instead of being strictly integer, as proposed in the previous research studies [12–16]. Such fractional domain analysis has been found to be necessary because the electrical circuit components in practice have irreversible dissipative effects, e.g., Ohmic friction, thermal memory, and electromagnetic field-induced nonlinearities, which cannot be precisely analyzed by using the conventional integer domain methods. Mostly, the linear electrical circuits have been considered despite the fact that there exists nonlinear ones which employ various interesting properties, e.g., chaotic behaviors. Among various nonlinear circuits, Chua's chaotic circuits [17–20], which employ interesting applications, e.g., secure communication system [21] and brain dynamic simulator [22], have been found to be often cited as they employ chaotic behaviors even though realizable by using very simple devices [19]. Therefore, their fractional domain generalizations have been proposed in many literatures [23–25]. Unfortunately, the dimensional consistency [26], which is often cited in many recent studies on the fractional domain linear circuit generalizations [27–29], has been neglected.

By this motivation, we perform the fractional domain generalization of Chua's chaotic circuit in this work by also considering such formerly ignored dimensional consistency. Similar to [23], the original simplest Chua's chaotic circuit [20], which is composed of only three electrical components, i.e., capacitor, inductor, and memristor, has been considered. In addition, the novel simplest chaotic circuit proposed by Jin et.al. [30], which can be thought of as the parallel

structured counterpart of Chua's simplest chaotic circuit, has also been considered. The analyses of the generalized circuits have been performed based on Jumarie's modified Riemann–Liouville fractional derivative [31] and nonlinear transformation [32] where the Lyapunov exponents and dimensions have also been calculated. Such derivative has been chosen despite the fact that there exist recent fractional derivatives, e.g., Caputo and Fabrizio [33] and Atangana and Baleanu fractional derivatives [34], because these new derivatives have been found to be controversial. As an example, it has been stated in [35] that these nonsingular kernel fractional derivatives are actually not derivatives. Moreover, they are also less accurate than the conventional fractional derivative in practice [36].

We have found that the dimensional consistency awareness significantly alters the dynamic; thus, the chaotic behavior of the fractional domain Chua's circuit from that of the previous dimensional consistency ignored the counterpart [23]. This is because different Lyapunov exponents and dimension can be obtained. The conditions for both fractional domain circuits which cease to be chaotic have also been determined where such condition of Chua's study is different from that of the previous work. This is because the time dimensionalconsistency has been included. The dynamical analyses of these circuits including Hopf bifurcation analyses have also been performed where their conditions for being nonchaotic have been verified, and it has been found that both circuits have undergone Hopf bifurcation through their equilibrium points. In addition, their emulators have also been realized.

In the following section, overview of the modified Riemann–Liouville fractional derivative will be briefly given followed by the introduction of the simplest Chua's chaotic circuit and the novel simplest one in Sections 3 and 4. The proposed fractional domain generalizations of the circuit will be shown in Section 5 where the corresponding dynamical analysis will also be presented. Finally, the conclusion will be drawn in Section 6.

2. Overview of the Modified Riemann–Liouville Fractional Derivative

In 2006, Jumarie proposed a modified version of Riemann–Liouville fractional derivative [31]. The proposed derivative can be mathematically defined as follows [31, 32].

Definition 1. Let $f(t)$ be arbitrary function of t where $t \in \mathfrak{R}$ and $0 \le \alpha \le 1$ where $\alpha \in \mathfrak{R}$, $D_t^\alpha f(t)$ can be given by

$$D_t^\alpha f(t) = \begin{cases} \dfrac{1}{\Gamma(-\alpha)} \displaystyle\int_0^t (t-\eta)^{-\alpha-1} [f(\eta) - f(0)] \mathrm{d}\eta, & \alpha < 0; \\ \dfrac{1}{\Gamma(1-\alpha)} \dfrac{\mathrm{d}}{\mathrm{d}t} \displaystyle\int_0^t (t-\eta)^{-\alpha} [f(\eta) - f(0)] \mathrm{d}\eta, & 0 < \alpha < 1; \\ \left(f^n(t)\right)^{(\alpha-n)}, & n \le \alpha \le n+1, n \ge 1, \end{cases} \tag{1}$$

where D_t^α stands for the fractional derivative operator of order α with respected to t. Obviously, the modified Riemann–Liouville fractional derivative obeys fundamental rules of conventional calculus, e.g., chain rule and product rule [32]. The Laplace transformation of this modified fractional derivative depends on α. As an example, $L[D_t^\alpha f(t)]$ when $1 < \alpha \le 2$ can be given by $L[D_t^\alpha f(t)] = s^\alpha L[f(t)] - s^{\alpha-1} f(0) - s^{\alpha-2} f'(0)$[31].

3. The Simplest Chua's Chaotic Circuit

In 2010, Muthuswamy and Chua proposed a chaotic circuit which was composed of merely three circuit elements, i.e., a capacitor, an inductor, and a memristor [20], connected in a series fashion. The proposed circuit has been found to be the simplest one among Chua's family of chaotic circuits. It is even simpler than its predecessor as proposed by Barboza and Chua in 2008 [19] which composes of four elements, i.e., two capacitors, an inductor, and a nonlinear resistor. Therefore, it has been found to be of interest. The schematic diagram of simplest Chua's chaotic circuit is depicted in Figure 1.

Moreover, it has been assumed that the memristor employs the following state equation and memristance:

$$\begin{aligned} \frac{\mathrm{d}}{\mathrm{d}t} x(t) &= -Ax(t) - i_M(t)x(t) + i_M(t), \\ M\Big(x(t) &= B(x(t))^2 - 1\Big), \end{aligned} \tag{2}$$

where $x(t)$, $M(x(t))$, A, and B denote the state variable, the memristance, and the memristor's parameters, respectively. Moreover, $i_M(t)$ stands for the memristor's current.

As a result, the following model of the simplest Chua's chaotic circuit can be obtained after performing a rigorous circuit analysis:

$$\begin{aligned} \frac{\mathrm{d}}{\mathrm{d}t} x(t) &= -Ax(t) + i_L(t)x(t) - i_L(t), \\ \frac{\mathrm{d}}{\mathrm{d}t} i_L(t) &= -\frac{1}{L}\left[B\Big((x(t))^2 - 1\Big) i_L(t) + v_C(t)\right], \\ \frac{\mathrm{d}}{\mathrm{d}t} v_C(t) &= \frac{i_L(t)}{C}, \end{aligned} \tag{3}$$

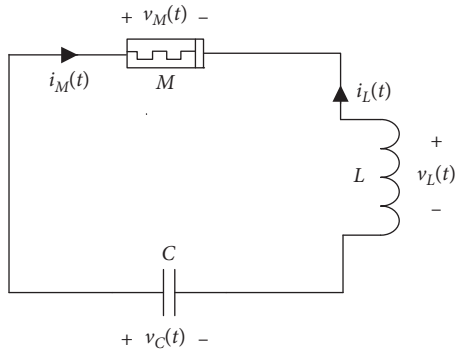

Figure 1: The simplest Chua's chaotic circuit [20].

where C, L, $i_L(t)$, and $v_C(t)$ denote the capacitance value, inductance value, current flowing through the inductor, and voltage drop across the capacitor, respectively. Note also that $i_L(t) = i_C(t) = -i_M(t)$. Before proceeding further, it should be mentioned here that the simplest Chua's chaotic circuit model exhibits the chaotic behaviors if and only if certain conditions on parameter values, e.g., $A = 0.2A$, $B = 1.7\,\Omega$, $L = 3.3H$, and $C = 1F$, have been met. Otherwise, other behaviors such as periodic and quasiperiodic will be encountered instead.

4. The Novel Simplest Chaotic Circuit

Later, Jin et.al. proposed a novel simplest chaotic circuit in 2018 [30]. Unlike that of Chua, this circuit is composed of a capacitor, an inductor, and a memristor connected in a parallel fashion as depicted in Figure 2; thus, it can be thought of as the parallel structured counterpart of the simplest Chua's circuit.

According to [30], the memristor employs the following state equation:

$$\frac{\mathrm{d}}{\mathrm{d}t}x(t) = a_1 x(t) + a_3 x^3(t) + b_1 v_m(t) + c_{11} v_m(t) x(t), \tag{4}$$

$$W(x(t)) = k\left(x^2(t) - x(t) - 1\right), \tag{5}$$

where a_1, a_3, b_1, c_{11}, and $v_m(t)$ are the memristor parameters and voltage. In addition, $W(x(t))$ stands for the memductance of the memristor [30].

Based on (3) and (4), the following model of the novel simplest chaotic circuit can be obtained:

$$\begin{aligned}
\frac{\mathrm{d}}{\mathrm{d}t}v_C(t) &= -\frac{1}{C}\left[k\left(x^2(t) - x(t) - 1\right)v_C(t) + i_L(t)\right],\\
\frac{\mathrm{d}}{\mathrm{d}t}i_L(t) &= \frac{1}{L}v_C(t),\\
\frac{\mathrm{d}}{\mathrm{d}t}x(t) &= a_1 x(t) + a_3 x^3(t) + b_1 v_C(t) + c_{11} v_C(t) x(t).
\end{aligned} \tag{6}$$

Note that $v_L(t) = v_C(t) = \mathrm{E}$. Similar to Chua's circuit, this novel circuit also exhibits chaotic behaviors if and only if certain conditions on parameter values have been met. Moreover, certain condition on the initial values must have been satisfied as well for obtaining the chaotic behavior [30].

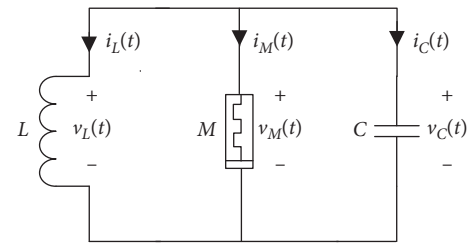

Figure 2: The novel simplest chaotic circuit [30].

5. The Fractional Domain Generalization

5.1. The Simplest Chua's Circuit. For generalizing the simplest Chua's chaotic circuit in the fractional domain, its conventional electrical circuit components, i.e., capacitor, inductor, and memristor, must be replaced by the fractional ones, i.e., fractional capacitor, fractional inductor, and fractional memristor, which can be emulated by simply replacing the conventional capacitor of the memristor emulator [20] by the fractional one. Mathematically, this is to replace all conventional derivatives in (3) by the fractional domain counterparts. In [23], such replacement has been directly performed without any awareness of the dimensional consistency as the time dimension of D_t^α is $\sec^{-\alpha}$ while that of $(\mathrm{d}/\mathrm{d}t)$ is $\sec^{-1}$. Moreover, $\sec^{-\alpha}$ is not physically measurable unlike $\sec^{-1}$. As a result, the following model of the fractional domain generalized simplest Chua's chaotic circuit can be obtained [23]:

$$\begin{aligned}
D_t^\alpha x(t) &= -Ax(t) + i_L(t)x(t) - i_L(t),\\
D_t^\alpha i_L(t) &= -\frac{1}{L}\left[B\left((x(t))^2 - 1\right)i_L(t) + v_C(t)\right],\\
D_t^\alpha v_C(t) &= \frac{i_L(t)}{C},
\end{aligned} \tag{7}$$

where $0 \le \alpha \le 1$ and $i_L(t) = i_C(t) = -i_M(t)$. Obviously, (7) is simply (3) with fractional derivatives.

However, this is not the case for this research as the dimensional consistency has been concerned unlike those previous works. For achieving the dimensional consistency, the time dimensions of $(\mathrm{d}/\mathrm{d}t)$ and the generalized fractional derivative must be consistent which means that both of them must be given by the physically measurable $\sec^{-1}$. Therefore, the following operation must be used:

$$\frac{\mathrm{d}}{\mathrm{d}t} \longrightarrow \frac{1}{\sigma^{1-\alpha}} D_t^\alpha, \tag{8}$$

where σ denotes the fractional time component or the cosmic time [26]. Note that $\sigma > 0$ always for preventing singularity. In addition, the introduction of σ scales only the Laplace transformed derivative term where the frequency scaling scales all complex frequency variables.

Since the dimension of σ is sec, that of $(1/\sigma^{1-\alpha})D_t^\alpha$ is also sec as the dimension of D_t^α is $\sec^{-\alpha}$ as stated above. Therefore, the dimensions of $(\mathrm{d}/\mathrm{d}t)$ and generalized fractional derivative, i.e., $(1/\sigma^{1-\alpha})D_t^\alpha$, are now consistent. As a result, the dimensional consistency of the generalized fractional domain model can be now achieved. Note also that (8) which has been adopted in those previous works on the fractional domain generalization of linear circuit models has been found to be suitable for our work since the assumed modified Riemann–Liouville fractional derivative employs a power law kernel as can be seen from (1). By using (8), we have

$$\begin{aligned}
\frac{1}{\sigma^{1-\alpha}}D_t^\alpha x(t) &= -Ax(t) + i_L(t)x(t) - i_L(t),\\
\frac{1}{\sigma^{1-\alpha}}D_t^\alpha i_L(t) &= -\frac{1}{L}\left[B\left((x(t))^2 - 1\right)i_L(t) + v_C(t)\right],\\
\frac{1}{\sigma^{1-\alpha}}D_t^\alpha v_C(t) &= \frac{i_L(t)}{C},
\end{aligned} \tag{9}$$

where $0 < \alpha \le 1$ and $i_L(t) = i_C(t) = -i_M(t)$.

After some rearrangement, we obtain

$$\begin{aligned}
D_t^\alpha x(t) &= -A_\alpha[x(t) + u(t)x(t) - u(t)],\\
D_t^\alpha u(t) &= -\frac{1}{L_\alpha}\left[B\left((x(t))^2 - 1\right)u(t) + v(t)\right],\\
D_t^\alpha v(t) &= \frac{u(t)}{C_\alpha},
\end{aligned} \tag{10}$$

where $A_\alpha = (A/\sigma^{\alpha-1})$, $C_\alpha = C\sigma^{\alpha-1}$, $L_\alpha = L\sigma^{\alpha-1}$, $u(t) = (i_L(t)/A)$, and $v(t) = (v_C(t)/A)$. Note also that C_α and L_α are generally known as the pseudocapacitance [37] of the fractional capacitor and the inductivity [38] of the fractional inductor, respectively. Obviously, (10), which is resulted by the dimensional consistency aware generalization, is significantly different from (7) as it is not merely (3) with fractional derivatives.

By some mathematical manipulation, (11) can be rewritten in a matrix-vector format as

$$D_t^\alpha \mathbf{x}(t) = \widehat{\mathbf{A}}(\mathbf{x}(t), t)\mathbf{x}(t), \tag{11}$$

where

$$\mathbf{x}(t) = \begin{bmatrix} x(t)\\ u(t)\\ v(t)\end{bmatrix},$$

$$\widehat{\mathbf{A}}(\mathbf{x}(t), t) = \begin{bmatrix} -A_\alpha & -A_\alpha(x(t) - 1) & 0\\ 0 & -\dfrac{B}{L_\alpha}\left((x(t))^2 - 1\right) & -\dfrac{1}{L_\alpha}\\ 0 & \dfrac{1}{C_\alpha} & 0\end{bmatrix}. \tag{12}$$

In this work, the fractional derivative has been interpreted in the modified Riemann–Liouville sense as given by (1); thus, we have

$$\mathbf{x}(t) = \frac{1}{\Gamma(1-\alpha)}\int_0^t (t-\tau)^{-\alpha-1}[\widehat{\mathbf{A}}(\mathbf{x}(\tau), \tau)\mathbf{x}(\tau) - \widehat{\mathbf{A}}(\mathbf{x}(0), 0)\mathbf{x}(0)]\mathrm{d}\tau. \tag{13}$$

For analyzing the generalized fractional dimensional consistency aware simplest Chua's chaotic circuit via simulations, its model given by (11) must be solved in a numerical manner. In order to do so, we apply the nonlinear transformation [32] to (13). As a result, we have

$$\frac{\mathrm{d}}{\mathrm{d}\xi}\mathbf{X}(\xi) = \widehat{\mathbf{A}}(\mathbf{X}(\xi), \xi)\mathbf{X}(\xi), \tag{14}$$

i.e.,

$$\mathbf{X}(\xi) = \mathbf{X}(0) + \int_0^\xi \widehat{\mathbf{A}}(\mathbf{X}(z), z)\mathbf{X}(z)\mathrm{d}z, \tag{15}$$

where

$$\mathbf{X}(\xi) = \begin{bmatrix} X(\xi)\\ U(\xi)\\ V(\xi)\end{bmatrix},$$

$$\widehat{\mathbf{A}}(\mathbf{X}(\xi), \xi) = \begin{bmatrix} -A_\alpha & -A_\alpha(X(\xi) - 1) & 0\\ 0 & -\dfrac{B}{L_\alpha}\left(X(\xi)^2 - 1\right) & -\dfrac{1}{L_\alpha}\\ 0 & \dfrac{1}{C_\alpha} & 0\end{bmatrix}. \tag{16}$$

Note also that $\mathbf{x}(t) = \mathbf{X}(\xi)$ where $\xi = (t^\alpha/\Gamma(1+\alpha))$ [32]. At this point, it can be seen that (11) has been transformed to (14). Therefore, the solution of (11) can be conveniently obtained by solving (14) and keeping the above relationships between $\mathbf{x}(t)$ and $\mathbf{X}(\xi)$ in mind. Here, we let $A = 0.2A$, $B = 1.7\,\Omega$, $L = 3.3H$, and $C = 1F$ similar to [20]. We also assume that $\alpha = 0.9$, $\sigma = 1$ sec, $X(0) = 0.1$, $U(0) = 0$, and $V(0) = 0.1\,\Omega$ and numerically solve (14) with MATHEMATICA with the above relationship between ξ and t in mind. As a result, the phase portraits of $x(t)$, $i_L(t)$, and $v_C(t)$ can be simulated by also keeping in mind that $i_L(t) = \mathrm{A}u(t)$ and $v_C(t) = Av(t)$ as depicted in Figures 3–5, where the strange attractors, which refers to the chaotic behaviors, can be observed.

For the quantitative analysis, we evaluate the corresponding Lyapunov exponents and Lyapunov dimension (D_L) by employing the following definition.

Definition 2. For any modified Riemann–Liouville fractional derivative-based fractional order dynamical system defined by

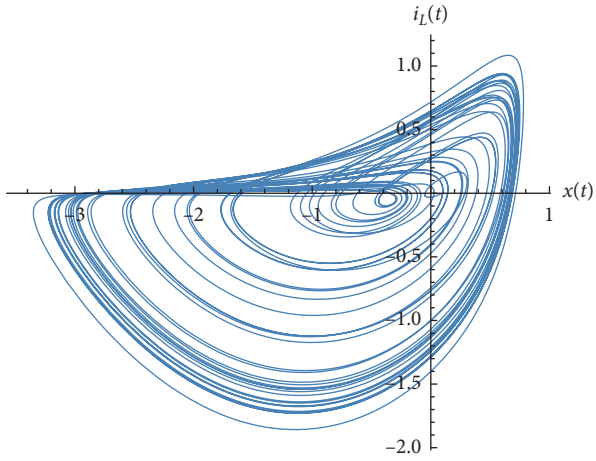

Figure 3: $i_L(t)$ vs $x(t)$ (Chua's circuit).

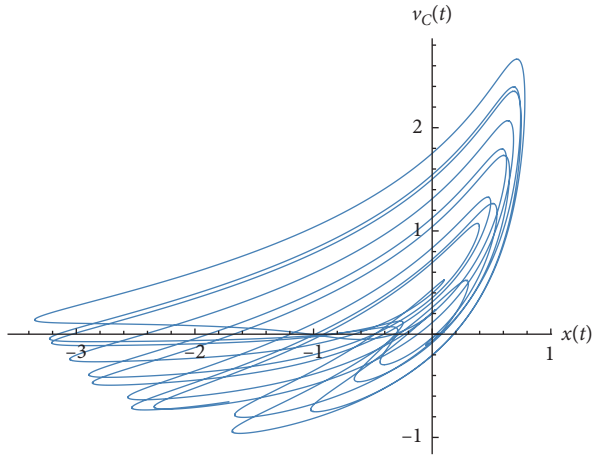

Figure 4: $v_C(t)$ vs $x(t)$ (Chua's circuit).

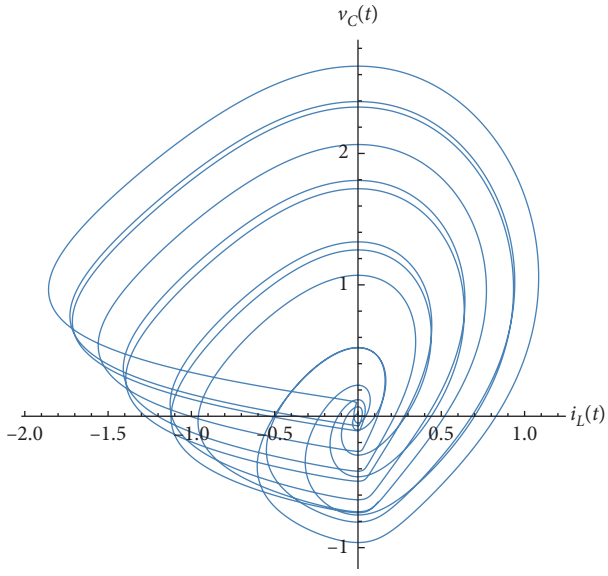

Figure 5: $v_C(t)$ vs $i_L t$ (Chua's circuit).

$$D_t^{\alpha}\mathbf{x}(t) = \mathbf{g}(\mathbf{x}(t)), \tag{17}$$

where

$$\mathbf{x}(t) = \left[\, x_1(t) \;\; x_2(t) \;\; \ldots \;\; x_N(t) \,\right]^T,$$

$$\mathbf{g}(\mathbf{x}(t)) = \begin{bmatrix} g_1(x_1(t), x_2(t), \ldots, x_N(t)) \\ g_2(x_1(t), x_2(t), \ldots, x_N(t)) \\ \vdots \\ g_N(x_1(t), x_2(t), \ldots, x_N(t)) \end{bmatrix}, \tag{18}$$

its jth Lyapunov exponent (λj) can be found as

$$\lambda_j = \lim_{\xi \longrightarrow \infty} \frac{1}{\xi} \ln\left[\frac{\left\|\mathbf{u}_j(\xi)\right\|}{\left\|\mathbf{u}_j(0)\right\|}\right], \tag{19}$$

where $\{j\} = \{1, 2, \ldots, N\}$ and $\mathbf{u}_j(\xi)$ stands for the j^{th} tangent vector of the system's trajectory in a ξ domain N dimensional space defined by $(X_1(\xi), X_2(\xi), \ldots, X_N(\xi))$. Note also that $X_j(\xi) = x_j(t)$, $\|\|$ denotes the Euclidian norm operator, and $\mathbf{u}_j(\xi)$ can be obtained by simultaneously solving the nonlinear transformed of (17) and its variational equation.

Obviously, Definition 2 states that all λ_j's and D_L of the modified Riemann–Liouville fractional derivative based system can be determined in a similar manner to that of the conventional integer order system after a nonlinear transformation. As a result, it has been found by using (14), the algorithm proposed by Sandri [39] and MATHEMATICA, that $\lambda_1 = 0.0473804$, $\lambda_2 = -0.0255304$, and $\lambda_3 = -0.550074$. Since $\lambda_1 > 0$ and $\lambda_1 + \lambda_2 + \lambda_3 = -0.528224$ which is less than 0, both expansion in one direction and contracting volumes in the phase space of the attractor that indicate the chaotic behavior. We have also found that the contraction outweighs the expansion as $\lambda_1 + \lambda_2 + \lambda_3 < 0$; therefore, our system is dissipative. Moreover, it has been found that $D_L = 2.03972$ which is a fractional number. Therefore, the manifold in the phase space is a strange attractor which indicates the chaotic behavior.

In order to demonstrate the significance of time dimensional consistency awareness, we compare our quantitative analysis results to their dimensional consistency ignored counterparts analyzed by using (7). For ceteris paribus and the applicability of Definition 2 thus Sandri's algorithm, all fractional derivative terms of (7) have also been defined in the modified Riemann–Liouville sense, unlike [23] in which the Caputo fractional derivative has been adopted. Moreover, the similar parameters except σ have been used. As a result, we have found that $\lambda_1 = 0.0202319$, $\lambda_2 = -0.000902803$, $\lambda_3 = -0.437888$, i.e., $\lambda_1 + \lambda_2 + \lambda_3 = -0.418559$, and $D_L = 2.04414$. These Lyapunov exponents and D_L are significantly different from those of the dimensional consistency aware scenario. Therefore, it can be seen that the fractional domain circuit employs different dynamic thus different chaotic behavior when the time dimensional consistency has been concerned. This is because

different amounts of expansion and contraction along with the fractal dimension phase space manifolds of the circuit can be obtained. It can also be seen that the dimensional consistency included the fractional circuit which became more dissipative than its dimensional consistency neglected predecessor as the latter employs lower $\lambda_1 + \lambda_2 + \lambda_3$. Also, unlike the previous dimensional consistency ignored circuit which is ceased to be chaotic if $\alpha < 0.715$ [23], a different condition on α can be obtained when the dimensional consistency is concerned. For illustration, we derive such condition that our dimensional consistency aware circuit ceases to be chaotic based on the same parameters as those of [23]. Firstly, the Jacobian matrix at equilibrium of the circuit's dynamical equation must be formulated by using the following definition.

Definition 3. For any fractional order dynamical system, its Jacobian matrix at arbitrary equilibrium point given by $E = (x_{1E}, x_{2E}, \ldots, x_{NE})$ ($\boldsymbol{J}_E$) can be defined as

$$\mathbf{J}_E = \left[\begin{array}{cccc} \frac{\partial g_1}{\partial x_1} & \frac{\partial g_1}{\partial x_2} & \cdots & \frac{\partial g_1}{\partial x_N} \\ \frac{\partial g_2}{\partial x_1} & \frac{\partial g_2}{\partial x_2} & \cdots & \frac{\partial g_2}{\partial x_N} \\ \frac{\partial g_3}{\partial x_1} & \frac{\partial g_3}{\partial x_2} & \cdots & \frac{\partial g_3}{\partial x_N} \\ \frac{\partial g_4}{\partial x_1} & \frac{\partial g_4}{\partial x_2} & \cdots & \frac{\partial g_4}{\partial x_N} \end{array}\right]_E. \tag{20}$$

Since this circuit has only one equilibrium point which can be given in terms of 3-tuples, i.e., $(x(t), u(t), v(t))$, by $E = (0, 0, 0)$, the resulting $\boldsymbol{J}_E$ can be obtained as follows:

$$\mathbf{J}_E = \left[\begin{array}{ccc} -A_\alpha & A_\alpha & 0 \\ 0 & \frac{B}{L_\alpha} & \frac{-1}{L_\alpha} \\ 0 & \frac{1}{C_\alpha} & 0 \end{array}\right]. \tag{21}$$

After obtaining $\boldsymbol{J}_E$, the characteristic equation can be determined by using the following corollary.

Corollary 1. *For arbitrary dynamical system, its characteristic equation can be given by*

$$\det\left[l\mathbf{I} - \mathbf{J}_E\right] = 0, \tag{22}$$

where l and $\boldsymbol{I}$ denote the eigenvalue symbol and the identity matrix.

As a result, the characteristic equation can be obtained based on (22) as

$$\det\left[\begin{array}{ccc} l + A_\alpha & -A_\alpha & 0 \\ 0 & \frac{l - B}{L_\alpha} & \frac{1}{L_\alpha} \\ 0 & \frac{-1}{C_\alpha} & l \end{array}\right] = 0, \tag{23}$$

which yields

$$\begin{aligned} l_1 &= -A_\alpha, \\ l_2 &= \frac{B}{2L_\alpha} + j\frac{\sqrt{4L_\alpha C_\alpha - \left(BC_\alpha\right)^2}}{L_\alpha C_\alpha}, \\ l_3 &= \frac{B}{2L_\alpha} - j\frac{\sqrt{4L_\alpha C_\alpha - \left(BC_\alpha\right)^2}}{L_\alpha C_\alpha}. \end{aligned} \tag{24}$$

For obtaining the chaotic behavior, E must be a saddle point of index 2 which generates the chaos in any three-dimensional system [40]. Thus, it can be seen from (24) that the following equation [41]

$$\alpha \leq \frac{2}{\pi}\tan^{-1}\left[\frac{\sqrt{4L_\alpha C_\alpha - \left(BC_\alpha\right)^2}}{BC_\alpha}\right], \tag{25}$$

must be satisfied for our circuit ceases to be chaotic. This is because the stable region of the complex plane has been enlarged so that it covers l_1, l_2, and l_3; thus, E becomes locally asymptotically stable. Based on the assumed parameters, we have $\alpha \leq 0.690015$ for our dimensional consistency aware scenario which is different from the above condition of the dimensional consistency ignored circuit.

Apart from satisfying (25), the circuit also ceases to be chaotic if $B \leq 0$ because both formerly unstable complex conjugate eigenvalues, i.e., l_2 and $l_3 l_2$ and l_3, will be resided in the stable region as $\mathrm{Re}[l_{2,3}] \leq 0$ regardless of α. Moreover, the conditions on L_α and C_α with which the circuit ceases to be chaotic can be obtained by using (24) as follows:

$$L_\alpha \geq \frac{B^2 C_\alpha}{4}\left(1 + \tan^2\left[\frac{\alpha\pi}{2}\right]\right), \tag{26}$$

$$C_\alpha \leq \frac{4L_\alpha}{B^2\left(1 + \tan^2\left[\alpha\pi/2\right]\right)}, \tag{27}$$

where α can be arbitrary. By satisfying either of these conditions, E becomes locally asymptotically stable as both l_2 and l_3 will be moved to the stable region. Therefore, all eigenvalues now reside in the stable region (as long as $A > 0$, which yields $A_\alpha > 0$, is satisfied, l_1 will always be located on the positive real axis of the complex plane) and the circuit ceases to be chaotic. If we let $A = 0.2A$, $B = 1.7\ \Omega$, $\alpha = 0.9$, and $\sigma = 1$ sec, (26) and (27) will become $L_\alpha \geq 29.5238\ \mathrm{Hsec}^{\alpha-1}$ for $C = 1F$ and $C_\alpha \leq 0.111774\ \mathrm{Fsec}^{\alpha-1}$ for $L = 3.3H$, respectively.

In order to verify the above conditions and study the dynamic of E which governs that of the circuit with respect to the changes in circuit parameters, we formulate

$$m_i = \frac{\alpha\pi}{2} - \left|\arg\left[l_i\right]\right|, \tag{28}$$

where $\{i\} = \{1, 2, 3\}$. It should be mentioned here that α, L_α, and C_α have been chosen as the bifurcation parameters and the effect of m_i to the location of l_i which governs the system dynamic is similar to that of the real part of l_i if l_i is an eigenvalue of the integer system [42]. Since the plots of real parts of eigenvalues with respect to bifurcation parameters have been adopted for studying the dynamic of conventional integer system in previous works [43, 44], the plots of m_i can be similarly used for studying the dynamic of the circuit despite that it is of fractional order. By using (24) and (28), we have

$$m_1 = \left(\frac{\alpha}{2} - 1\right)\pi, \tag{29}$$

$$m_{2,3} = \frac{\alpha\pi}{2} - \tan^{-1}\left[\frac{\sqrt{4L_\alpha C_\alpha - \left(BC_\alpha\right)^2}}{BC_\alpha}\right]. \tag{30}$$

As a result, the dynamics of m_1 and $m_{2,3}$ can be simulated as follows.

It can be seen from Figures 6–8 that $m_1 < 0$ always unlike m_2 and m_3 depicted in Figures 9–11. Thus, the circuit's stability is solely governed by l_2 and l_3 as l_1 will always be in the stable region of the complex plane. The circuit becomes asymptotically stable if and only if $\alpha < 0.690015$, $L_\alpha > 29.5238\,\text{Hsec}^{\alpha-1}$, and $C_\alpha < 0.111774\,\text{Fsec}^{\alpha-1}$ have been assured because $m_{2,3} < 0$ which implies that l_2 and l_3 are in the stable region and can be observed. Otherwise, $m_{2,3} > 0$ which implies that l_2 and l_3 are in the unstable region; thus, the circuit becomes unstable and can be seen instead. The circuit becomes marginally stable when either $\alpha = 0.690015$, $L_\alpha = 29.5238\,\text{Hsec}^{\alpha-1}$ or $C_\alpha = 0.111774\,\text{Fsec}^{\alpha-1}$ has been satisfied since $m_{2,3} = 0$ can be found. This verifies (25)–(27) as the circuit becomes nonchaotic in these scenarios. In addition, we have found that the transversality condition is established at $\alpha = 0.690015$, $L_\alpha = 29.5238\,\text{Hsec}^{\alpha-1}$, and $C_\alpha = 0.111774\,\text{Fsec}^{\alpha-1}$ because

$$\begin{aligned}
\frac{\partial}{\partial\alpha}m_{2,3}\bigg|_{\alpha=0.690015} &= \frac{\pi}{2} \neq 0,\\
\frac{\partial}{\partial L_\alpha}m_{2,3}\bigg|_{L_\alpha=29.5238} &= -0.00268232 \neq 0,\\
\frac{\partial}{\partial C_\alpha}m_{2,3}\bigg|_{C_\alpha=0.111774} &= 0.708053 \neq 0,
\end{aligned} \tag{31}$$

where $m_{2,3} = 0$ as stated above. Moreover, we have also found that the real eigenvalue can be given by $l_1 = -0.2\,\text{A/sec}^{\alpha-1} \neq 0$ in these circumstances. As a result, the Hopf bifurcation condition for arbitrary three-dimensional fractional order system [42] has been satisfied. Thus, it can be stated that the circuit's stability switches and the circuit undergo a Hopf bifurcation through E when either $\alpha = 0.690015$, $L_\alpha = 29.5238\,\text{Hsec}^{\alpha-1}$ or $C_\alpha = 0.111774\,\text{Fsec}^{\alpha-1}$ has been satisfied. As an illustration, the phase portraits of $i_L(t)$ and $v_C(t)$ with $L_\alpha = 29.5238\,\text{Hsec}^{\alpha-1}$ can be simulated as depicted in Figure 12, where a limit cycle, which indicates a periodic solution, can be observed. It should be mentioned here that such Hopf bifurcation cannot occur when $\alpha \neq 0.690015$, $L_\alpha \neq 29.5238\,\text{Hsec}^{\alpha-1}$, and $C_\alpha \neq 0.111774\,\text{Fsec}^{\alpha-1}$ despite the fact that $l_1 \neq 0$ is satisfied (since $l_1 = -0.2\,\text{A/sec}^{\alpha-1}$ is always based on the assumed parameter according to (24)). This is because $m_{2,3} \neq 0$ as can be seen from Figures 7, 9, and 11.

Before proceeding further, it should be mentioned here that our dimensional consistency aware fractional domain Chua's circuit cannot be realized by simply replacing the capacitor, the inductor, and the memristor by the fractional ones. This is because (10) is not merely (3) with fractional derivatives. However, (10) can be rewritten in terms of fractional integrals as

$$\begin{aligned}
x(t) &= -A_\alpha J_t^\alpha\left[x(t) + u(t)x(t) - u(t)\right],\\
u(t) &= -\frac{1}{L_\beta}J_t^\beta\left[B\left((x(t))^2u(t) - u(t)\right) + v(t)\right],\\
v(t) &= \frac{1}{C_\gamma}J_t^\gamma u(t),
\end{aligned} \tag{32}$$

where J_t^α, J_t^β, and J_t^γ, respectively, denote the fractional integral operators of order α, β, and γ with respect to t. Note that the order of the fractional derivative terms has been allowed to be incommensurate for obtaining full degree of freedom; thus, L_α and C_α must become L_β and C_γ, which can be, respectively, given by $L_\beta = L\sigma^{\beta-1}$ and $C_\gamma = C\sigma^{\gamma-1}$, where $0 < \beta \leq 1$ and $0 < \gamma \leq 1$ for maintaining the dimensional consistency. By using (32), the emulator of our dimensional consistency aware circuit can be obtained generically without referring to any specific physical system as depicted in Figure 13. Based on this generic emulator, the specific circuit emulator can be obtained by using merely the shelf components. An example of such circuit emulator is depicted in Figure 14. Moreover, $x(t)$, $u(t)$, and $v(t)$ are in terms of voltages. Note also that this circuit emulates the conventional simplest Chua's chaotic circuit if all fractional capacitors have been replaced by the conventional ones. From Figure 14, it can be seen that the OPAMPs and fractional capacitors have been used for realizing the fractional integrators; AD633, which is off the shelf analog voltage multiplier, has been adopted for performing multiplication and the OPAMP-based unity gain inverting amplifiers have been used as the invertors. Here, we choose TL084 as our OPAMP.

For realizing the fractional capacitors, we firstly approximate the impedance function of fractional capacitor generally given by $Z_\delta(s) = C_\delta^{-1}s^{-\delta}$ where $C_\delta = C\sigma^{\delta-1}$ and $0 < \delta \leq 1$ as follows [45]:

$$C_\delta^{-1}s^{-\delta} \approx K + \sum_{i=1}^{N}\left[\frac{L_i}{s + M_i}\right], \tag{33}$$

where N can be arbitrary positive integer. Thus, the circuit that approximates the fractional capacitor which is solely composed of resistors and capacitors which are off the shelf components can be obtained as depicted in Figure 15, where

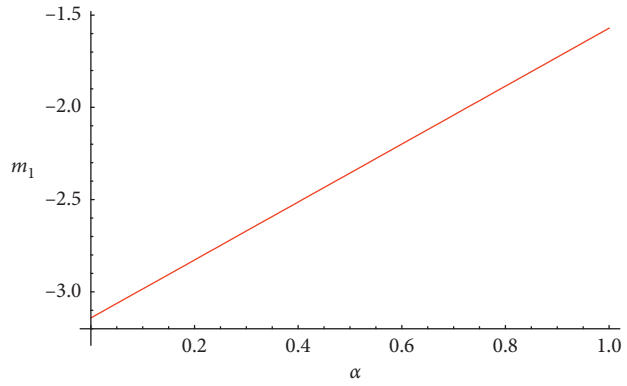

Figure 6: m_1 vs α.

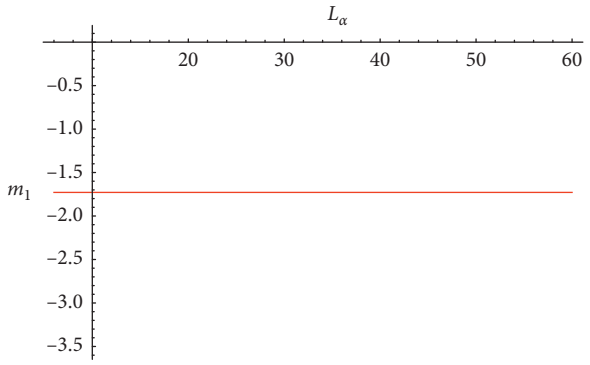

Figure 7: m_1 vs L_α.

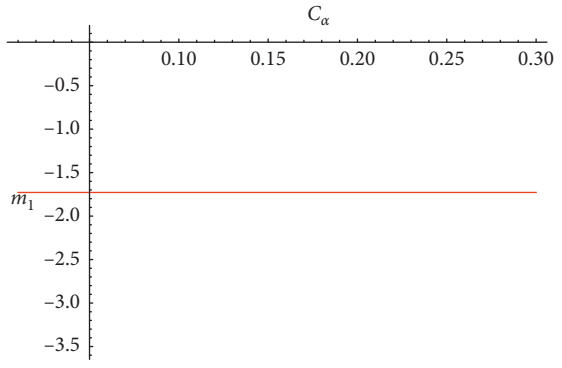

Figure 8: m_1 vs C_α.

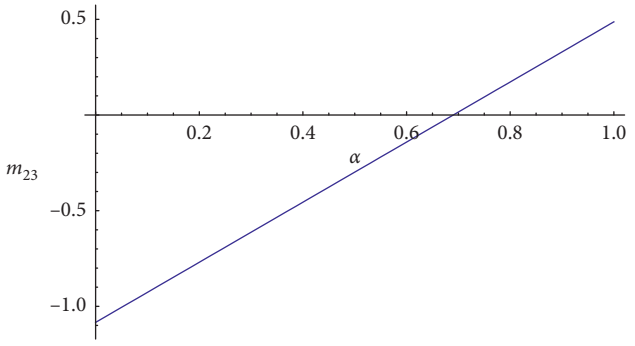

Figure 9: $m_{2,3}$ vs α.

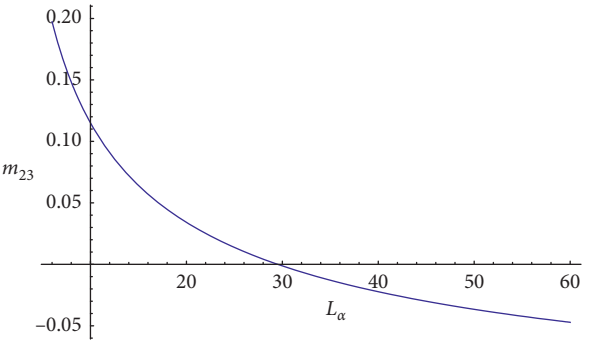

Figure 10: $m_{2,3}$ vs L_α.

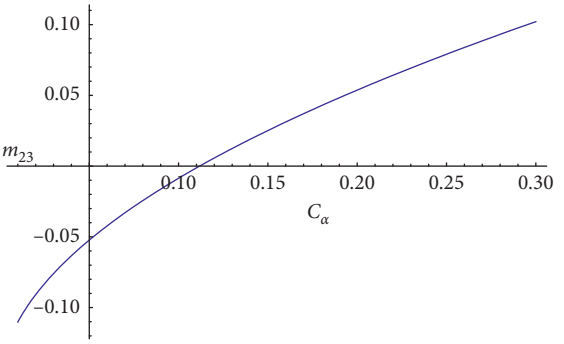

Figure 11: $m_{2,3}$ vs C_α.

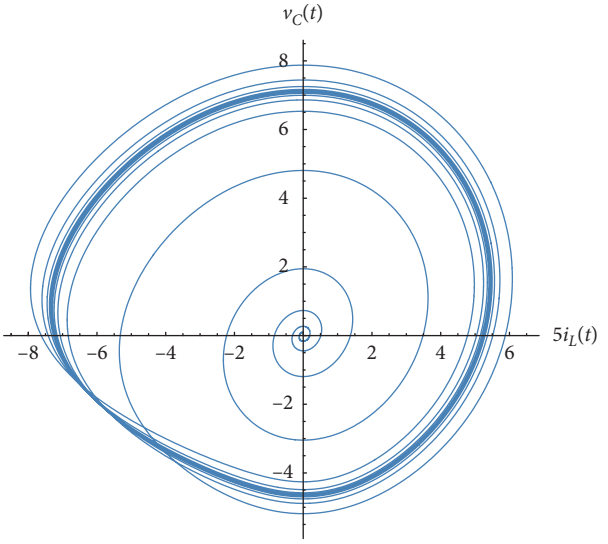

Figure 12: $v_C(t)$ vs $i_L(t)$ ($L_\alpha = 29.5238\ \text{Hsec}^{\alpha-1}$).

$R_0 = K$, $R_i = L_i/M_i$, and $C_i = 1/L_i$. It should be mentioned here that K, L_i's, and M_i's can be computed by using the method of undetermined coefficients [45]. As a practical example, a circuit that approximates a fractional capacitor with $C_\delta = 1\ \mu\text{Fsec}^{\delta-1}$ and $\delta = 0.9$ can be realized by assuming that $N = 3$ as the RC approximated circuit with 3 R//C stages composed of $R_0 = 1\ \text{M}\Omega$, $R_1 = 62.84\ \text{M}\Omega$, $R_2 = 250\ \text{k}\Omega$, $R_3 = 2.5\ \text{k}\Omega$, $C_1 = 1.23\ \mu\text{F}$, $C_2 = 1.835\ \mu\text{F}$ and $C_3 = 1.1\ \mu\text{F}$. If we let $\sigma = 1$ sec, $A = 0.2A$, $L = 3.3H$, $C = 1F$, $B = 1.7S$, $x(0) = 0.1$ V,

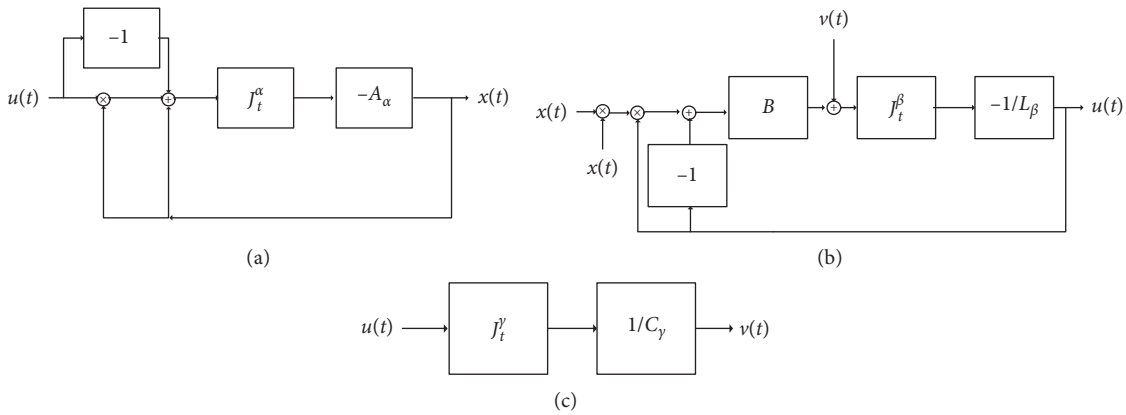

Figure 13: The generic emulator of dimensional consistency aware fractional domain Chua's circuit.

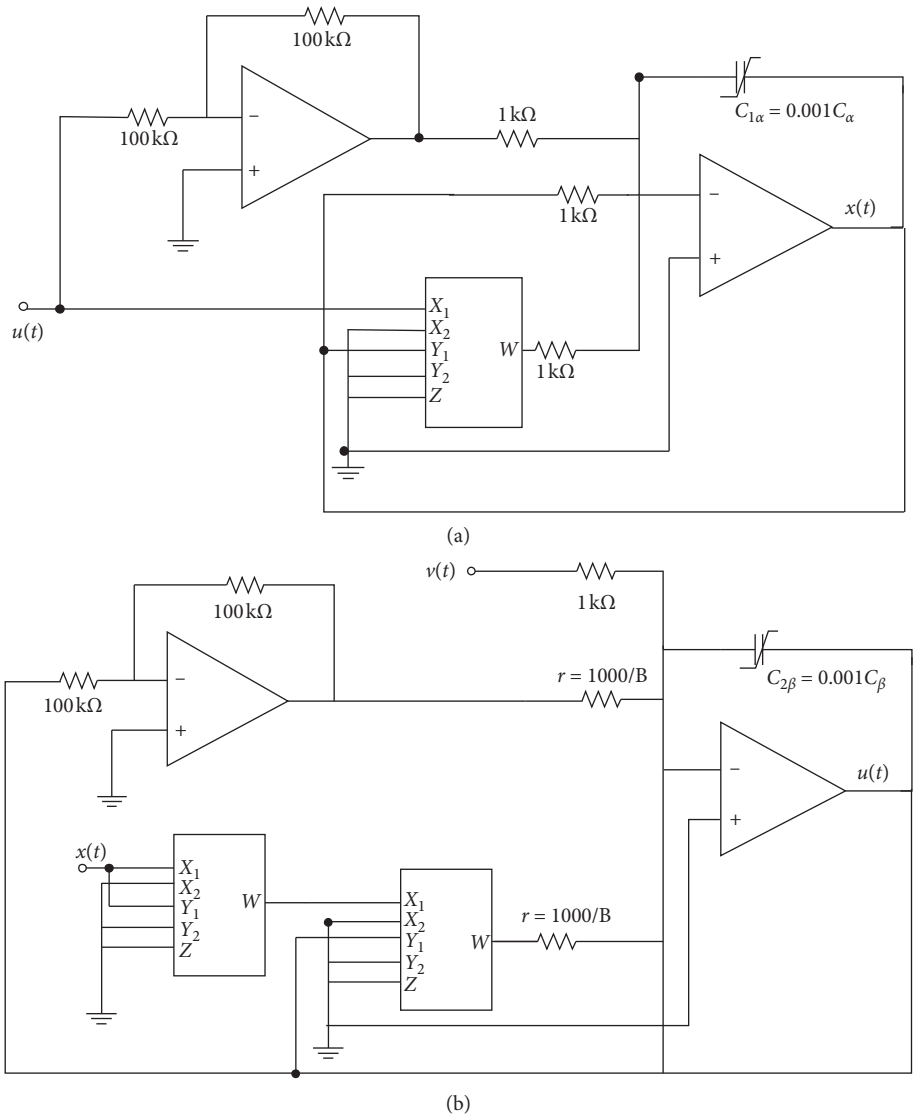

Figure 14: Continued.

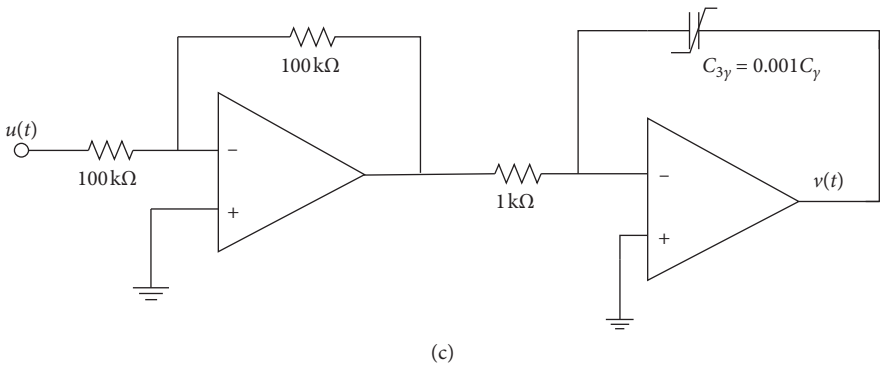

Figure 14: An example of specific circuit implementation of the emulator depicted in Figure 13.

$u(0) = 0$ V, $v(0) = 0.1$ V, $\alpha = 0.8$, and $\beta = 0.95$, $\gamma = 0.85$, the phase portraits of $x(t)$, $0.2u(t)$, and $0.2v(t)$ can be simulated by using PSPICE which has been adopted in many previous works [40, 45] as depicted in Figures 16–18. Note that $N = 7$ has been assumed because the resulting approximated RC circuit with such N yields the results which are as accurate as the 7^{th} order Oustaloup approximation-based results [45]. The parameter values of this circuit emulator can be summarized in Table 1 where the OPAMP's supply voltage (V_{sup}) of ± 15 V has been adopted.

5.2. The Novel Simplest Circuit. Now, the novel simplest chaotic circuit will be considered. After the fractional domain generalization, we have

$$\frac{1}{\sigma^{1-\alpha}} D_t^{\alpha} v_C(t) = -\frac{1}{C}\left[k\left(x^2(t) - x(t) - 1\right)v_C(t) + i_L(t)\right],$$

$$\frac{1}{\sigma^{1-\alpha}} D_t^{\alpha} i_L(t) = \frac{1}{L} v_C(t),$$

$$\frac{1}{\sigma^{1-\alpha}} D_t^{\alpha} x(t) = a_1 x(t) + a_3 x^3(t) + b_1 v_C(t) + c_{11} v_C(t) x(t). \tag{34}$$

By defining $a_{1\alpha} = a_1 \sigma^{1-\alpha}$, $a_{3\alpha} = a_3 \sigma^{1-\alpha}$, $b_{1\alpha} = b_1 \sigma^{1-\alpha}$, and $c_{11\alpha} = c_{11} \sigma^{1-\alpha}$ the following dimensional consistency aware fractional domain model of the simplest paralleled structured chaotic circuit can be obtained.

$$D_t^{\alpha} v_C(t) = -\frac{1}{C_{\alpha}}\left[k\left(x^2(t) - x(t) - 1\right)v_C(t) + i_L(t)\right],$$

$$D_t^{\alpha} i_L(t) = \frac{1}{L_{\alpha}} v_C(t),$$

$$D_t^{\alpha} x(t) = a_{1\alpha} x(t) + a_{3\alpha} x^3(t) + b_{1\alpha} v_C(t) + c_{11\alpha} v_C(t) x(t). \tag{35}$$

After some rearrangement, the matrix vector formatted of (35) can be given as follows:

$$D_t^{\alpha} \mathbf{y}(t) = \widehat{\mathbf{B}}(\mathbf{y}(t), t)\mathbf{y}(t), \tag{36}$$

where

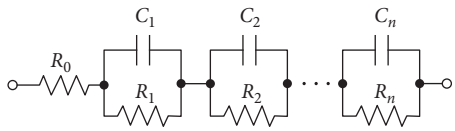

Figure 15: The RC circuit approximation of fractional capacitor [45].

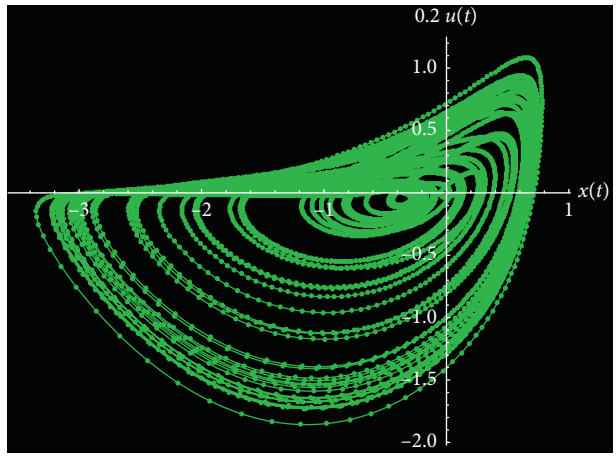

Figure 16: $0.2u(t)$ vs $x(t)$.

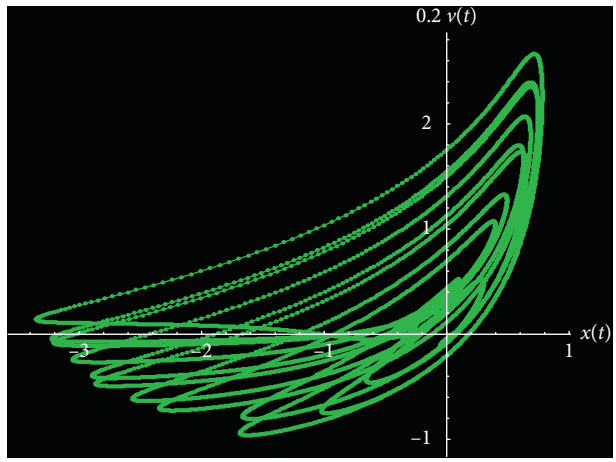

Figure 17: $0.2v(t)$ vs $x(t)$.

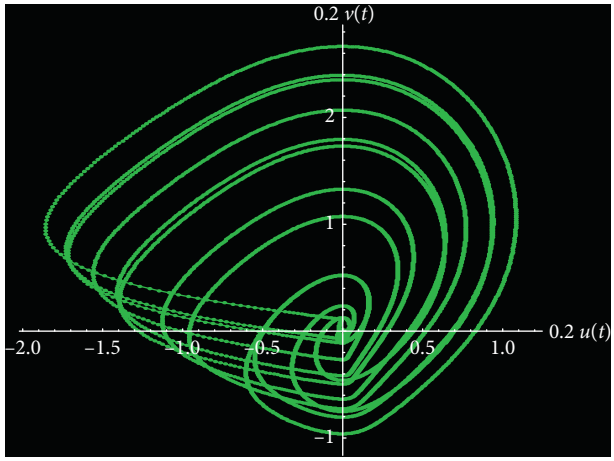

Figure 18: $0.2v(t)$ vs $0.2u(t)$.

Table 1: Parameter values of the circuit emulator depicted in Figure 14.

Parameter	Value
r	588 Ω
$C_{1\alpha}$	5 mFsec$^{\alpha-1}$
$C_{2\beta}$	3.3 mFsec$^{\beta-1}$
$C_{3\gamma}$	1 mFsec$^{\gamma-1}$
α	0.8
β	0.95
γ	0.85
V_{supply}	±15 V

$$\mathbf{y}(t) = \begin{bmatrix} v_C(t) \\ i_L(t) \\ x(t) \end{bmatrix},$$

$$\widehat{\mathbf{B}}(\mathbf{y}(t), t) = \begin{bmatrix} -\frac{k}{C_\alpha}\left(x^2(t) - x(t) - 1\right) & -\frac{1}{C_\alpha} & 0 \\ \frac{1}{L_\alpha} & 0 & 0 \\ b_{1\alpha} + c_{11\alpha}x(t) & 0 & a_{1\alpha} + a_{3\alpha}x^2(t) \end{bmatrix}. \tag{37}$$

Since the fractional derivative has been interpreted in the modified Riemann–Liouville sense, we have

$$\mathbf{y}(t) = \frac{1}{\Gamma(1-\alpha)} \int_0^t (t-\tau)^{-\alpha-1} [\widehat{\mathbf{B}}(\mathbf{y}(\tau), \tau)\mathbf{y}(\tau) - \widehat{\mathbf{B}}(\mathbf{y}(0), 0)\mathbf{y}(0)]\mathrm{d}\tau. \tag{38}$$

For solving (36) in a numerical manner, the nonlinear transformation has also been applied. As a result, we have

$$\frac{\mathrm{d}}{\mathrm{d}\xi}\mathbf{Y}(\xi) = \widehat{\mathbf{B}}(\mathbf{Y}(\xi), \xi)\mathbf{Y}(\xi), \tag{39}$$

i.e.,

$$\mathbf{Y}(\xi) = \mathbf{Y}(0) + \int_0^\xi \widehat{\mathbf{B}}(\mathbf{Y}(z), z)\mathbf{Y}(z)\mathrm{d}z, \tag{40}$$

where

$$\mathbf{Y}(\xi) = \begin{bmatrix} V_C(\xi) \\ I_L(\xi) \\ X(\xi) \end{bmatrix},$$

$$\widehat{\mathbf{B}}(\mathbf{Y}(\xi), \xi) = \begin{bmatrix} -\frac{k}{C_\alpha}\left(X^2(\xi) - X(\xi) - 1\right) & -\frac{1}{C_\alpha} & 0 \\ \frac{1}{L_\alpha} & 0 & 0 \\ b_{1\alpha} + c_{11\alpha}X(\xi) & 0 & a_{1\alpha} + a_{3\alpha}X^2(\xi) \end{bmatrix}. \tag{41}$$

Note also that $\mathbf{y}(t) = \mathbf{Y}(\xi)$. Similar to [30], we let $a_1 = 1.8$, $a_3 = -3.9$, $b_1 = 1.4$, $c_{11} = -1.5$, $k = 1$, $C = 130$ mF, $L = 50$ mH, $v_C(0) = 0.1$ V, $i_L(0) = 0.1A$, and $x(0) = 0.2$. We also assume that $\alpha = 0.9$ and $\sigma = 1$ sec and numerically solve (36). By using the obtained solutions and keeping the above relationship between $\mathbf{y}(t)$ and $\mathbf{Y}(\xi)$ along with that of ξ and t mentioned above in mind, the phase portraits of $x(t)$, $i_L(t)$, and $v_C(t)$ can be simulated as depicted in Figures 19–21, where the strange attractors can be observed. In addition, we have found that $\lambda_1 = 1.37332$, $\lambda_2 = -0.23593$, $\lambda_3 = -12.1655$, and $D_L = 2.09348$. Since $\lambda_1 > 0$, $\lambda_1 + \lambda_2 + \lambda_3 = -11.02811$, which is less than 0, and D_L is a fractional number, a dissipative chaotic behavior, which is even more dissipative than Chua's circuit analyzed in the previous section, can be observed. The Lyapunov exponents and dimensions of this circuit and Chua's circuit are summarized in Table 2.

Similar to the simplest Chua's circuit considered in the previous subsection, we also determine the condition on α in which this novel simplest circuit ceased to be chaotic. Unlike Chua's circuit, which employs only one equilibrium point, the novel simplest circuit employs three points which can be given in terms of $(v_C(t), i_L(t), x(t))$ as $E_1 = (0, 0, 0)$, $E_2 = (0, 0, \sqrt{-(a_{1\alpha}/a_{3\alpha})})$, and $E_3 = (0, 0, -\sqrt{-(a_{1\alpha}/a_{3\alpha})})$. Among these equilibrium points, only E_2 will be considered because such point implies that $x(0) \geq 0$ which guarantees the chaotic behavior of the circuit as the local activity of the memristive device can be assured [30]. As a result, the Jacobian matrix at E_2 can be given by following Definition 3 as

$$\mathbf{J}_{E_2} = \begin{bmatrix} \frac{k}{C_\alpha}\left(\frac{a_{1\alpha}}{a_{3\alpha}} + \sqrt{-\frac{a_{1\alpha}}{a_{3\alpha}}} + 1\right) & -\frac{1}{C_\alpha} & 0 \\ \frac{1}{L_\alpha} & 0 & 0 \\ b_{1\alpha} + c_{11\alpha}\sqrt{-\frac{a_{1\alpha}}{a_{3\alpha}}} & 0 & -2a_{1\alpha} \end{bmatrix}. \tag{42}$$

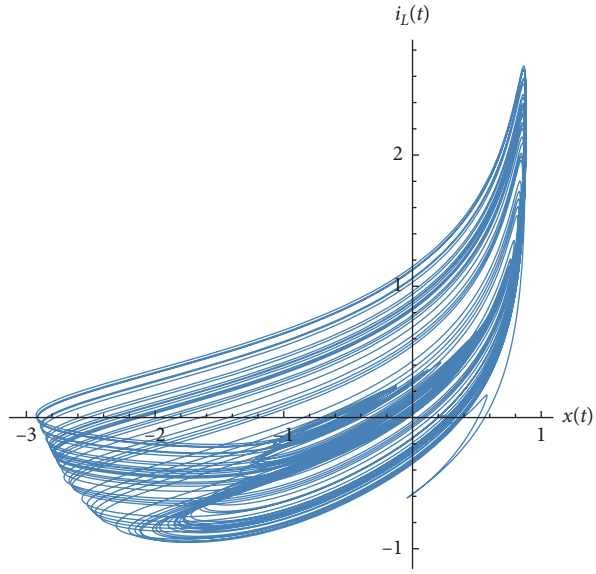

Figure 19: $i_L(t)$ vs $x(t)$ (novel circuit).

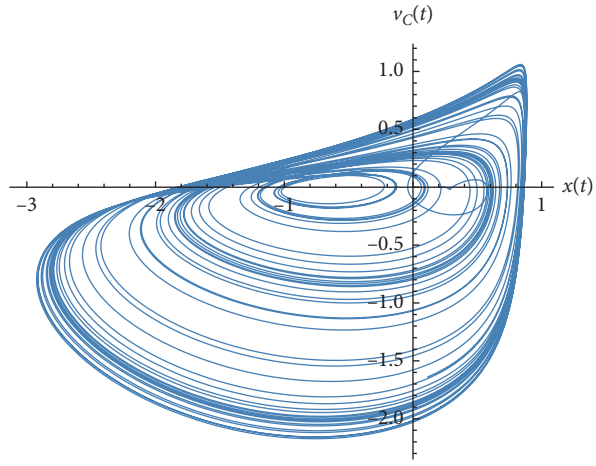

Figure 20: $v_C(t)$ vs $x(t)$ (novel circuit).

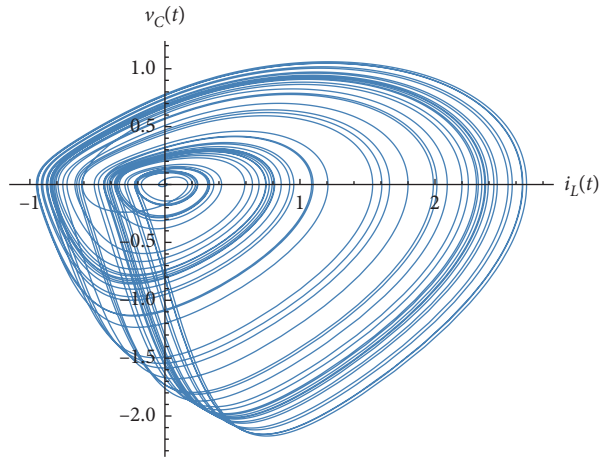

Figure 21: $v_C(t)$ vs $i_L(t)$ (novel circuit).

Table 2: Lyapunov exponents and dimensions.

Circuit	λ_1	λ_2	λ_3	$\lambda_1+\lambda_2+\lambda_3$	D_L
Chua's circuit	0.0473804	0.0255304	0.550074	−0.528224	2.03972
Chua's circuit (dimensional consistency ignored)	0.0202319	0.000902803	0.437888	−0.418559	2.04414
Novel circuit	1.37332	−0.23593	−12.1655	−11.02811	2.09348

Therefore, the characteristic equation can be obtained by following Corollary 1 as follows:

$$\det\begin{bmatrix} l-\dfrac{k}{C_\alpha}\left(\dfrac{a_{1\alpha}}{a_{3\alpha}}+\sqrt{-\dfrac{a_{1\alpha}}{a_{3\alpha}}}+1\right) & \dfrac{1}{C_\alpha} & 0 \\ -\dfrac{1}{L_\alpha} & l & 0 \\ -b_{1\alpha}-c_{11\alpha}\sqrt{-\dfrac{a_{1\alpha}}{a_{3\alpha}}} & 0 & l+2a_{1\alpha} \end{bmatrix}=0, \tag{43}$$

which yields

$$\begin{aligned} l_1 &= -2a_{1\alpha}, \\ l_2 &= \frac{k(a_{1\alpha}+a_{3\alpha})}{2a_{3\alpha}C_\alpha}+j\frac{ka_{1\alpha}L_\alpha+\sqrt{4a_{1\alpha}a_{3\alpha}C_\alpha L_\alpha+\left(k(a_{1\alpha}+a_{3\alpha})L_\alpha\sqrt{-a_{1\alpha}/a_{3\alpha}}-ka_{1\alpha}L_\alpha\right)^2}}{2\sqrt{a_{1\alpha}a_{3\alpha}}C_\alpha L_\alpha}, \\ l_3 &= \frac{k(a_{1\alpha}+a_{3\alpha})}{2a_{3\alpha}C_\alpha}-j\frac{ka_{1\alpha}L_\alpha+\sqrt{4a_{1\alpha}a_{3\alpha}C_\alpha L_\alpha+\left(k(a_{1\alpha}+a_{3\alpha})L_\alpha\sqrt{-a_{1\alpha}/a_{3\alpha}}-ka_{1\alpha}L_\alpha\right)^2}}{2\sqrt{a_{1\alpha}a_{3\alpha}}C_\alpha L_\alpha}. \end{aligned} \tag{44}$$

By using (44), we have found that the novel simplest chaotic circuit ceases to be chaotic if $(a_{1\alpha}+a_{3\alpha}/2a_{3\alpha\alpha})\le 0$ has been satisfied. This is because l_2 and l_3 will reside in the stable region of the complex plane. Moreover, this circuit also ceases to be chaotic if

$$\alpha\le\frac{2}{\pi}\tan^{-1}\left[-\frac{\left[4a_{3\alpha}^2L_\alpha C_\alpha-\left(a_{1\alpha}^2+a_{1\alpha}a_{3\alpha}+a_{3\alpha}^2+2(a_{1\alpha}+a_{3\alpha})\sqrt{-a_{1\alpha}a_{3\alpha}}\right)k^2L_\alpha^2\right]^{(1/2)}}{\left(a_{1\alpha}+a_{3\alpha}+\sqrt{-a_{1\alpha}a_{3\alpha}}\right)kL_\alpha}\right], \tag{45}$$

has been satisfied due to the aforementioned stable region enlargement. Based on the assumed parameters, we have found that $\alpha\le 0.75317$ must be satisfied for this novel circuit ceases to be chaotic.

In addition, we have also found that satisfying either (46) or (47) makes the novel circuit ceases to be chaotic despite the fact that (45) has not been satisfied. This is because l_2 and l_3 will be moved to the stable region. Here, we let $a_1=1.8$, $a_3=-3.9$, $b_1=1.4$, $c_{11}=-1.5$, $k=1$, $\sigma=1$ sec, and $\alpha=0.9$; therefore, (46) and (47) become $L_\alpha\le 8.58018\,\text{mHsec}^{\alpha-1}$ if $C=130\,\text{mF}$ and $C_\alpha\ge 757.56\,\text{mFsec}^{\alpha-1}$ if $L=50\,\text{mH}$, respectively.

$$L_\alpha\le\left[\frac{2a_{3\alpha}^2\left(a_{1\alpha}^2+a_{1\alpha}a_{3\alpha}+a_{3\alpha}^2+2(a_{3\alpha}-a_{1\alpha})\sqrt{-a_{1\alpha}a_{3\alpha}}+a_{3\alpha}^2\right)C(1+\cos[\alpha\pi])}{\left(a_{1\alpha}^2+3a_{1\alpha}a_{3\alpha}+a_{3\alpha}^2\right)^2k^2}\right], \tag{46}$$

$$C_\alpha\ge\frac{\left(a_{1\alpha}^2+(a_{1\alpha}+a_{3\alpha})\left(a_{3\alpha}+2\sqrt{-a_{1\alpha}a_{3\alpha}}\right)\right)k^2L_\alpha}{4a_{3\alpha}^2\cos^2[\alpha\pi/2]}. \tag{47}$$

At this point, we will study the dynamic of E_2 and the novel circuit and also verify the above conditions. For this circuit, it has been found that m_1 can also be given by (29) according to (44); thus, the dynamic of m_1 with respect to α similar to that depicted in Figure 6 can be obtained. On the other hand, $m_{2,3}$ can be found as

$$m_{2,3} = \frac{\alpha\pi}{2} - \tan^{-1}\left[-\frac{\left[4a_{3\alpha}^2 L_\alpha C_\alpha - \left(a_{1\alpha}^2 + a_{1\alpha}a_{3\alpha} + a_{3\alpha}^2 + 2\left(a_{1\alpha} + a_{3\alpha}\right)\sqrt{-a_{1\alpha}a_{3\alpha}}\right)k^2 L_\alpha^2\right]^{(1/2)}}{\left(a_{1\alpha} + a_{3\alpha} + \sqrt{-a_{1\alpha}a_{3\alpha}}\right)kL_\alpha}\right]. \tag{48}$$

As a result, the dynamics of m_1 with respect to other bifurcation parameters and those of $m_{2,3}$ can be simulated as depicted in Figures 22–26 which also imply that the circuit's stability is solely governed by l_2 and l_3. In this case, the circuit becomes asymptotically stable when either $\alpha < 0.75317$, $L_\alpha < 8.58018\,\text{Hsec}^{\alpha-1}$ or $C_\alpha > 757.56\,\text{Fsec}^{\alpha-1}$ has been assured and vice versa and become marginally stable when either $\alpha = 0.75317$, $L_\alpha = 8.58018\,\text{Hsec}^{\alpha-1}$ or $C_\alpha = 757.56\,\text{Fsec}^{\alpha-1}$ has been satisfied. This verifies (45)–(47) as the circuit becomes nonchaotic in these scenarios. On the other hand, the real eigenvalue can be given by $l_1 = -3.6\,\text{A/sec}^{\alpha-1} \neq 0$ along the entire ranges of bifurcation parameters because l_1 is constant with respect to these parameters as can be seen from (44). If at least one of the above marginal stability conditions on bifurcation parameters has been satisfied, we have $m_{2,3} = 0$ where

$$\begin{aligned}
\frac{\partial}{\partial\alpha}m_{2,3}\bigg|_{\alpha=0.75317} &= \frac{\pi}{2} \neq 0,\\
\frac{\partial}{\partial L_\alpha}m_{2,3}\bigg|_{L_\alpha=8.58018\times10^{-3}} &= 9.22967 \neq 0,\\
\frac{\partial}{\partial C_\alpha}m_{2,3}\bigg|_{C_\alpha=757.56\times10^{-3}} &= -0.104536 \neq 0,
\end{aligned} \tag{49}$$

and as a result, the transversality condition has been established; thus, the Hopf bifurcation condition has been satisfied. Therefore, the stability switches and the circuit undergoes a Hopf bifurcation through E_2 when either $\alpha = 0.75317$, $L_\alpha = 8.58018\,\text{Hsec}^{\alpha-1}$ or $C_\alpha = 757.56\,\text{Fsec}^{\alpha-1}$. As an illustration, the phase portraits of $i_L(t)$ and $v_C(t)$ with $C_\alpha = 757.56\,\text{Fsec}^{\alpha-1}$ can be simulated as depicted in Figure 27 where a limit cycle can be obtained. Note also that such bifurcation does not exist when $\alpha \neq 0.75317$, $L_\alpha \neq 8.58018\,\text{Hsec}^{\alpha-1}$, and $C_\alpha \neq 757.56\,\text{Fsec}^{\alpha-1}$ despite the fact that $l_1 \neq 0$. This is because $m_{2,3} \neq 0$ as can be seen from Figures 22, 24, and 26.

For implementing the emulator of the fractional domain simplest paralleled structured chaotic circuit, (35) must be firstly rewritten in terms of fractional integration. Since we let the order of the fractional derivative terms be incommensurate, L_α and C_α become L_γ and C_β. We also define $y(t) = v_C(t)$ and $z(t) = i_L(t)$. As a result, we have

$$\begin{aligned}
x(t) &= J_t^\alpha\left[a_{1\alpha}x(t) + a_{3\alpha}x^3(t) + b_{1\alpha}y(t) + c_{11\alpha}y(t)x(t)\right],\\
y(t) &= -\frac{1}{C_\beta}J_t^\beta\left[k\left(x^2(t)y(t) - x(t)y(t) - y(t)\right) + z(t)\right],\\
z(t) &= \frac{1}{L_\gamma}J_t^\gamma y(t).
\end{aligned} \tag{50}$$

Therefore, the resulting generic emulator can be obtained as depicted in Figure 28.

An example of circuit emulator implemented based on such generic one is depicted in Figure 29 where $x(t)$, $y(t)$, and $z(t)$ in terms of voltages and $C_{1\alpha} = 1\,\text{mFsec}^{\alpha-1}$ have been assumed. In addition, NR1 and NR_2 are floating negative resistors because $a_3 < 0$ and $c_{11} < 0$. These negative resistors have been realized by using OTA which is off the shelf component, by following [46], where the transconductances of these OTAs have been given by $g_{m1} = 0.001a_{3\alpha}$ and $g_{m2} = 0.001c_{11\alpha}$. The OPAMP-fractional capacitor-based fractional integrators, unity gain inverting amplifier, and AD633 multiplier have also been adopted. We also use TL084 as our OPAMP and the aforementioned RC approximated circuit with $N = 7$ for realizing the fractional capacitors. It should be mentioned here that this emulator emulates the novel simplest paralleled structured chaotic circuit when all fractional capacitors have been replaced by the conventional ones. If we let $\sigma = 1$ sec, $\alpha = 0.8$, $\beta = 0.95$, $\gamma = 0.85$, $a_1 = 1.8$, $a_3 = -3.9$, $b_1 = 1.4$, $c_{11} = -1.5$, $k = 1$, $C = 130$ mF, $L = 50$ mH, $x(0) = 0.2$ V, $y(0) = 0.1$ V, and $z(0) = 0.1$ V, the phase portraits of $x(t)$, $y(t)$, and $z(t)$ can be simulated by PSPICE as depicted in Figures 30–32. The circuit parameter values for realizing this emulator are summarized in Table 3 (±15 V DC supply voltage for each OPAMP has also been assumed).

6. Conclusion

The simplest Chua's chaotic circuit and its novel parallel structured counterpart have been generalized in the fractional domain with the dimensional consistency awareness for the first time in this work. The analysis has been performed where the chaotic behaviors can be observed. The conditions for both which cease to be chaotic have also been determined. With these conditions, the behaviors of the circuits can be controlled. We have found that the inclusion

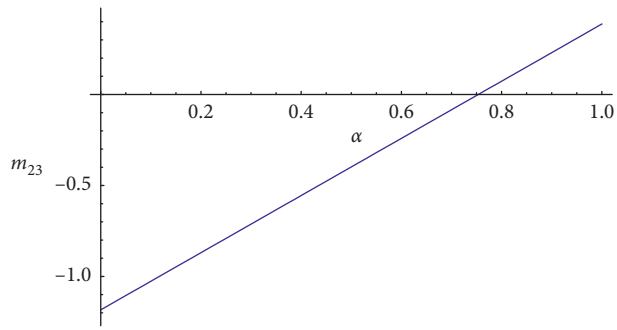

Figure 22: $m_{2,3}$ vs α.

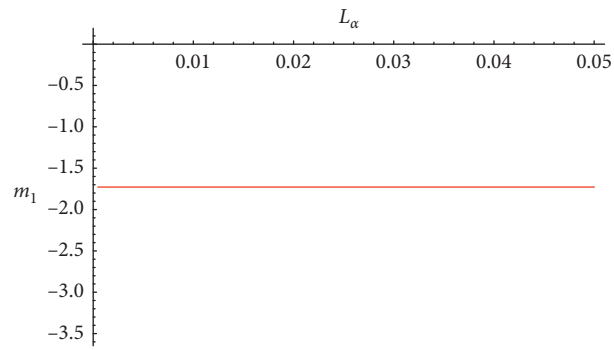

Figure 23: m_1 vs L_α.

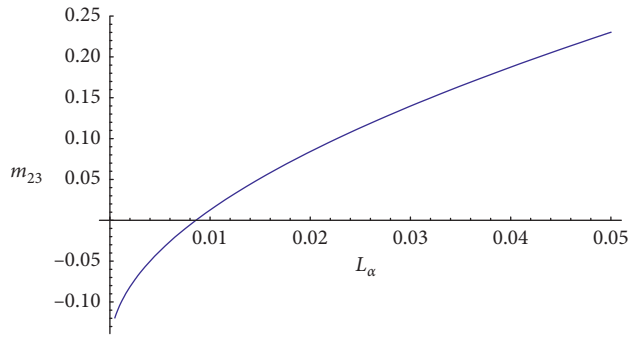

Figure 24: $m_{2,3}$ vs L_α.

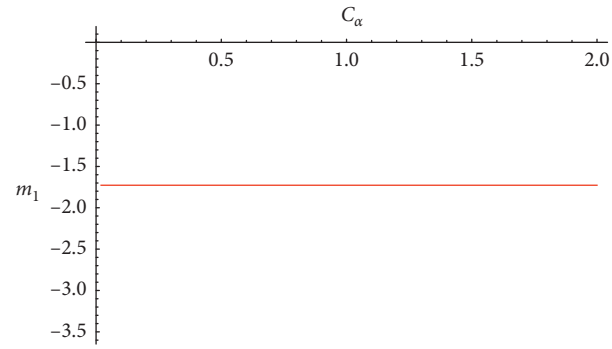

Figure 25: $m_{2,3}$ vs C_α.

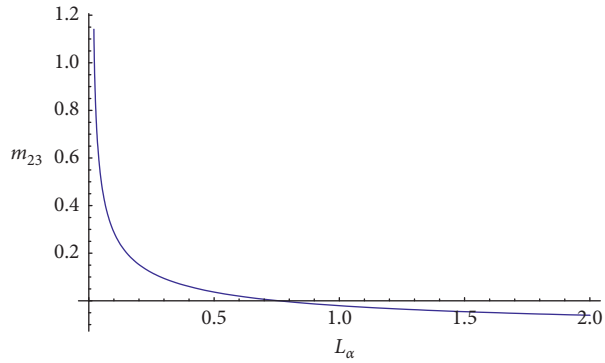

Figure 26: $m_{2,3}$ vs C_α.

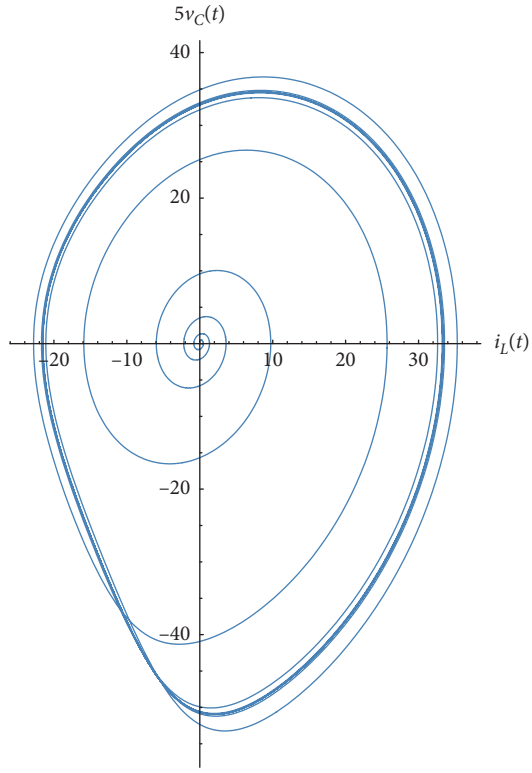

Figure 27: $v_C(t)$ vs $i_L(t)$ ($C_\alpha = 757.56\,\text{Fsec}^{\alpha-1}$).

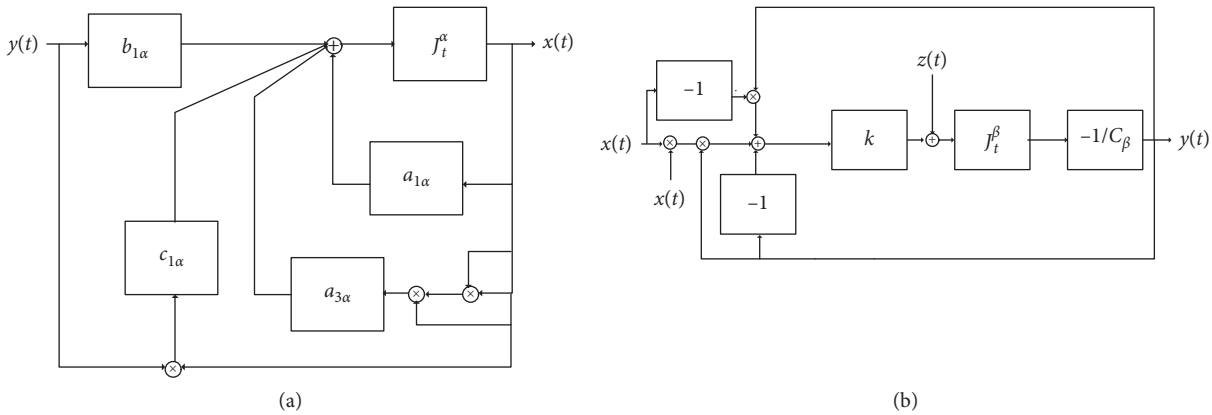

Figure 28: Continued.

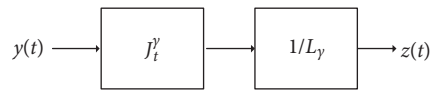

(c)

Figure 28: The generic emulator of the dimensional consistency aware simplest paralleled structured fractional domain chaotic circuit.

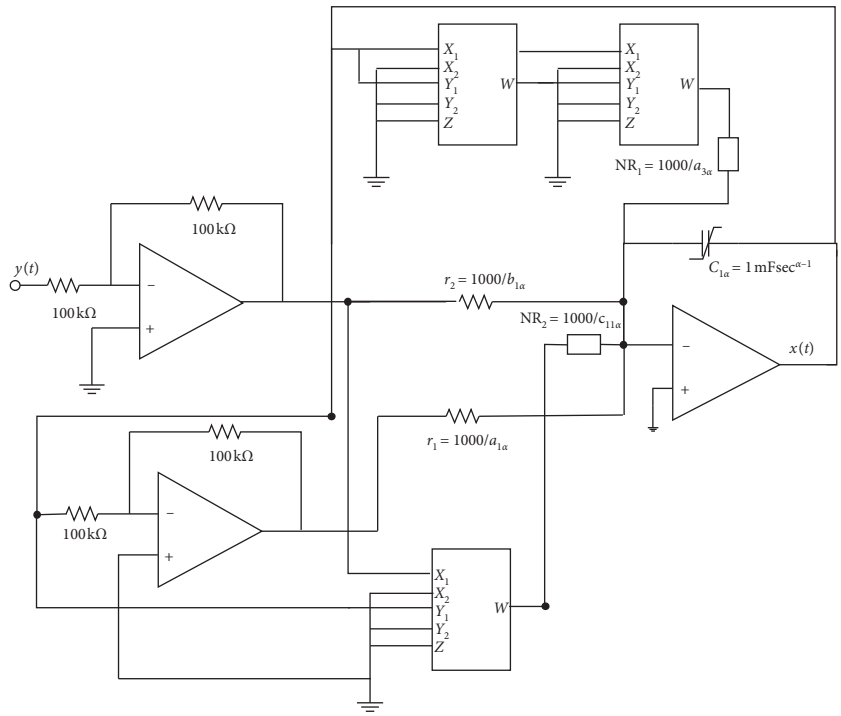

(a)

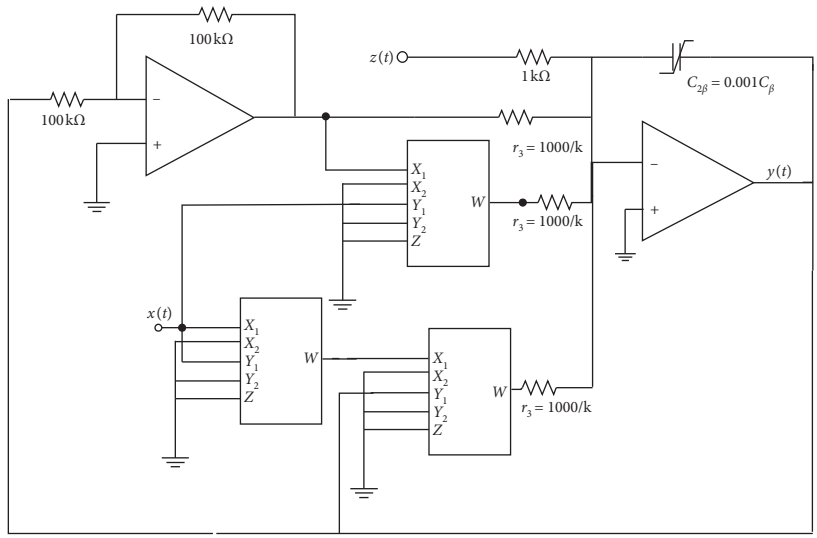

(b)

Figure 29: Continued.

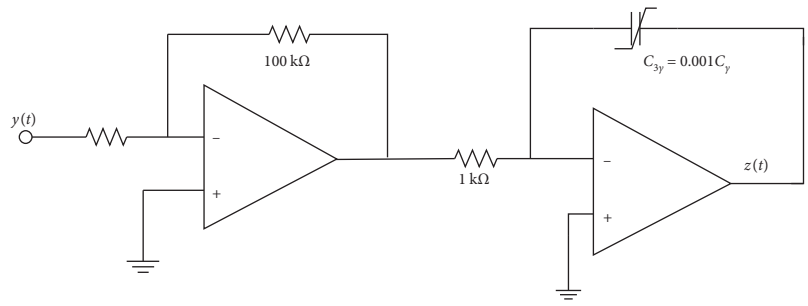

Figure 29: An example of specific circuit implementation of the emulator depicted in Figure 28.

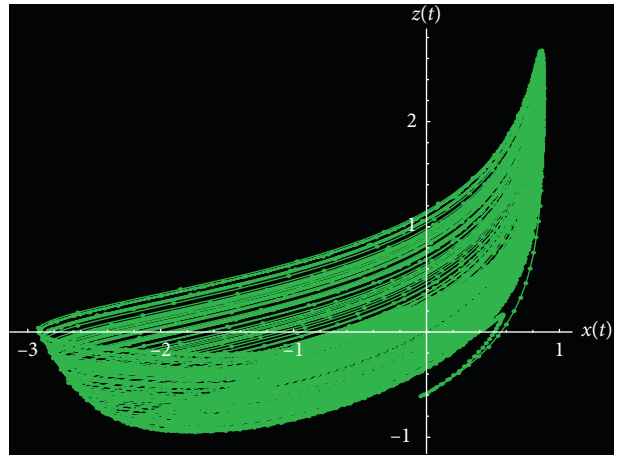

Figure 30: $z(t)$ vs $x(t)$.

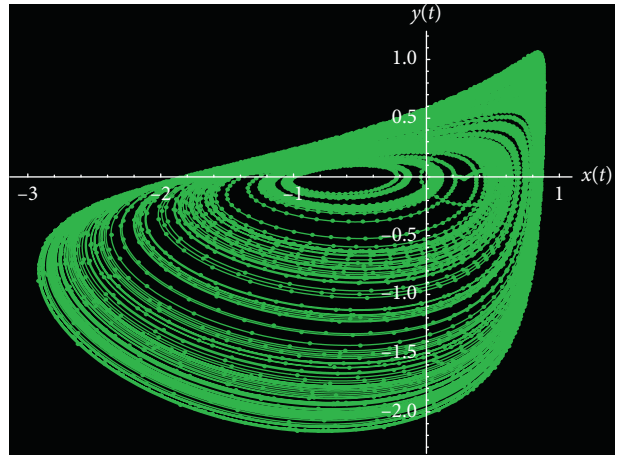

Figure 31: $y(t)$ vs $x(t)$.

of time dimensional consistency awareness significantly affects the behaviors of the fractional domain circuit. This is because different Lyapunov exponent spectra/dimension and condition for the circuit which cease to be chaotic can be obtained when such consistency awareness has been taken into account. The dynamical analyses including Hopf bifurcation analyses of these circuits have also been done where their conditions for being nonchaotic have been verified. It has been found that both circuits have undergone Hopf bifurcations through their equilibrium. Moreover, the their emulators have also been realized and simulated by PSPICE. At this point, it can be seen that this work has been

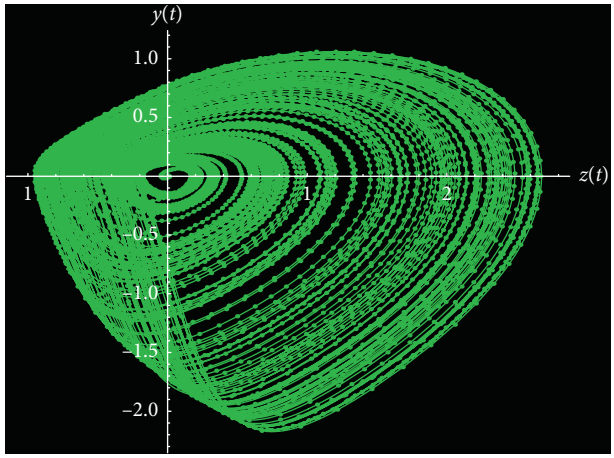

Figure 32: $y(t)$ vs $z(t)$.

Table 3: Parameter values of the circuit emulator depicted in Figure 29.

Parameter	Value
r_1	555.5 Ω
r_2	714.3 kΩ
r_3	1 kΩ
$C_{1\alpha}$	1 mFsec$^{\alpha-1}$
$C_{2\beta}$	130 μFsec$^{\beta-1}$
$C_{3\gamma}$	50 μFsec$^{\gamma-1}$
α	0.8
β	0.95
γ	0.85
g_{m1}	3.9 ms
g_{m2}	1.5 ms
V_{supply}	±15 V

found to be beneficial to the analysis and design of fractional chaotic circuit along with the related research areas.

Data Availability

The simulated data used to support the findings of this study are included within the article.

Conflicts of Interest

The author declares that there are no conflicts of interest regarding the publication of this article.

Acknowledgments

The author would like to acknowledge Mahidol University, Thailand, for the online database service which was the primary information resource.

References

[1] L. Sommacal, P. Melchior, A. Oustaloup, J.-M. Cabelguen, and A. J. Ijspeert, "Fractional multi-models of the frog gastrocnemius muscle," *Journal of Vibration and Control*, vol. 14, no. 9-10, pp. 1415–1430, 2008.

[2] J. Cervera and A. Baños, "Automatic loop shaping in QFT using CRONE structures," *Journal of Vibration and Control*, vol. 14, no. 9-10, pp. 1513–1529, 2008.

[3] R. Panda and M. Dash, "Fractional generalized splines and signal processing," *Signal Processing*, vol. 86, no. 9, pp. 2340–2350, 2006.

[4] L. Debnath, "Recent applications of fractional calculus to science and engineering," *International Journal of Mathematics and Mathematical Sciences*, vol. 2003, no. 54, pp. 3413–3442, 2003.

[5] R. L. Magin and M. Ovadia, "Modeling the cardiac tissue electrode interface using fractional calculus," *Journal of Vibration and Control*, vol. 14, no. 9-10, pp. 1431–1442, 2008.

[6] B. T. Krishna and K. V. V. S. Reddy, "Active and passive realization of fractance device of order 1/2," *Active and Passive Electronic Components*, vol. 2008, Article ID 369421, 5 pages, 2008.

[7] G. W. Bohannan, "Analog fractional order controller in temperature and motor control applications," *Journal of Vibration and Control*, vol. 14, no. 9-10, pp. 1487–1498, 2008.

[8] M. F. M. Lima, J. A. T. Machado, and M. Cris´ostomo, "Experimental signal analysis of robot impacts in a fractional calculus perspective," *JACIII*, vol. 11, pp. 1079–1085, 2007.

[9] Y. Pu, X. Yuan, K. Liao et al., "A recursive two-circuits series analog fractance circuit for any order fractional calculus," in *Proceedings of the ICO20: Optical Information Processing*, vol. 6027, pp. 509–519, Changchun, China, 2006.

[10] Z.-Z. Yang and J.-L. Zhou, "An improved design for the IIR-type digital fractional order differential filter," in *Proceedings of the 2008 International Seminar on Future BioMedical Information Engineering*, pp. 473–476, Wuhan, China, 2008.

[11] J. Rosario, D. Dumur, and J. T. Machado, "Analysis of fractional-order robot axis dynamics," in *Proceedings of the IFAC Proceedings Volumes*, vol. 39, no. 11, pp. 367–372, 2006.

[12] M. Guia, F. Gomez, and J. Rosales, "Analysis on the time and frequency domain for the RC electric circuit of fractional order," *Open Physics*, vol. 11, no. 10, pp. 1366–1371, 2013.

[13] G.-A. J. Francisco, R.-G. Juan, and R.-H. J Roberto, "Fractional RC and LC electrical circuits," *Ingeniería, Investigación y Tecnología*, vol. 15, no. 2, pp. 311–319, 2014.

[14] P. V. Shah, A. D. Patel, I. A. Salehbhai, and A. K. Shukla, "Analytic solution for the RL Electric circuit model in fractional order," *Abstract and Applied Analysis*, vol. 2014, Article ID 343814, 5 pages, 2014.

[15] F. Gómez, J. Rosales, and M. Guía, "RLC electrical circuit of non-integer order," *Open Physics*, vol. 11, no. 10, pp. 1361–1365, 2013.

[16] A. A. Rousan, N. Y. Ayoub, F. Y. Alzoubi et al., "A fractional LC–RC circuit," *Fractional Calculus and Applied Analysis*, vol. 9, pp. 33–41, 2006.

[17] L. O. Chua, "The genesis of Chua's circuit," *Archiv für Elektronik und Ubertragungstechnik*, vol. 46, pp. 250–257, 1992.

[18] L. O. Chua, "IEICE transactions on fundamentals of electronics," *Communications and Computer Sciences*, vol. 76, no. 5, pp. 704–734, 1993.

[19] R. Barboza and L. O. Chua, "The four-element Chua's circuit," *International Journal of Bifurcation and Chaos*, vol. 18, no. 4, pp. 943–955, 2008.

[20] B. Muthuswamy and L. O. Chua, "Simplest chaotic circuit," *International Journal of Bifurcation and Chaos*, vol. 20, no. 5, pp. 1567–1580, 2010.

[21] I. A. Kamil and O. A. Fakolujo, "Chaotic secure communication schemes employing Chua's circuit," in *Proceedings of*

the 17th International Conference on Systems, Signals and Image Processing-IWSSIP 2010, Rio de Janeiro, Brazil, 2010.

[22] P. L. Gentili, *Untangling Complex Systems: A Grand Challenge for Science*, CRC Press, Boca Raton, FL, USA, 2018.

[23] D. Cafagna and G. Grassi, "On the simplest fractional-order memristor-based chaotic system," *Nonlinear Dynamics*, vol. 70, no. 2, pp. 1185–1197, 2012.

[24] Y. Chunde, H. Cai, and P. Zhou, "Stabilization of the fractional-order chua chaotic circuit via the Caputo derivative of a single input," *Discrete Dynamics in Nature and Society*, vol. 2016, Article ID 4129756, 5 pages, 2016.

[25] B. S. T. Alkahtani, "Chua's circuit model with Atangana-Baleanu derivative with fractional order," *Chaos, Solitons & Fractals*, vol. 89, pp. 547–551, 2016.

[26] J. F. Gómez-Aguilar, J. J. Rosales-García, J. J. Bernal-Alvarado, T. Córdova-Fraga, and R. Guzmán-Cabrera, "Fractional mechanical oscillators," *Revista Mexicana de Física*, vol. 58, pp. 348–352, 2012.

[27] A. Atangana and B. S. T. Alkahtani, "Extension of the resistance, inductance, capacitance electrical circuit to fractional derivative without singular kernel," *Advances in Mechanical Engineering*, vol. 7, no. 6, 2015.

[28] J. F. Gómez-Aguilar, A. Atangana, and V. F. Morales-Delgado, "Electrical circuits RC, LC, and RL described by Atangana–Baleanu fractional derivatives," *International Journal of Circuit Theory and Applications*, vol. 45, no. 11, pp. 1514–1533, 2017.

[29] L. Martínez, J. J. Rosales, C. A. Carreño, and J. M. Lozano, "Electrical circuits described by fractional conformable derivative," *International Journal of Circuit Theory and Applications*, vol. 46, no. 5, pp. 1091–1100, 2018.

[30] P. Jin, G. Wang, H. H.-C. Iu, and T. Fernando, "A locally active memristor and its application in a chaotic circuit," *IEEE Transactions on Circuits and Systems II: Express Briefs*, vol. 65, no. 2, pp. 246–250, 2018.

[31] G. Jumarie, "Modified Riemann-Liouville derivative and fractional Taylor series of nondifferentiable functions further results," *Computers & Mathematics with Applications*, vol. 51, no. 9-10, pp. 1367–1376, 2006.

[32] G. M. Mahmoud, A. A. M. Farghaly, and A. A.-H. Shoreh, "A technique for studying a class of fractional-order nonlinear dynamical systems," *International Journal of Bifurcation and Chaos*, vol. 27, no. 9, Article ID 1750144, 2017.

[33] M. Caputo and M. Fabrizio, "A new definition of fractional derivative without singular kernel," *Progress in Fractional Differentiation and Applications*, vol. 1, pp. 73–85, 2015.

[34] A. Atangana and D. Baleanu, "New fractional derivatives with nonlocal and non-singular kernel: theory and application to heat transfer model," *Thermal Science*, vol. 20, no. 2, pp. 763–769, 2016.

[35] M. D. Ortigueira and J. Tenreiro Machado, "A critical analysis of the Caputo-Fabrizio operator," *Communications in Nonlinear Science and Numerical Simulation*, vol. 59, pp. 608–611, 2018.

[36] C. A. Carreño, J. J. Rosales, L. R. Merchan, J. M. Lozano, and F. A. Godínez, "Comparative analysis to determine the accuracy of fractional derivatives in modeling supercapacitors," *International Journal of Circuit Theory and Applications*, vol. 47, no. 10, pp. 1603–1614, 2019.

[37] T. J. Freeborn, B. Maundy, and A. S. Elwakil, "Measurement of supercapacitor fractional-order model parameters from voltage-excited step response," *IEEE Journal on Emerging and Selected Topics in Circuits and Systems*, vol. 3, no. 3, pp. 367–376, 2013.

[38] I. Schäfer and K. Krüger, "Modelling of coils using fractional derivatives," *Journal of Magnetism and Magnetic Materials*, vol. 307, no. 1, pp. 91–98, 2006.

[39] M. Sandri, "Numerical calculation of Lyapunov exponents," *Mathematica Journal*, vol. 6, no. 3, pp. 78–84, 1996.

[40] Z. Wang, X. Huang, and G. Shi, "Analysis of nonlinear dynamics and chaos in a fractional order financial system with time delay," *Computers & Mathematics with Applications*, vol. 62, no. 3, pp. 1531–1539, 2011.

[41] M. S. Tavazoei and M. Haeri, "Limitations of frequency domain approximation for detecting chaos in fractional order systems," *Nonlinear Analysis: Theory, Methods & Applications*, vol. 69, no. 4, pp. 1299–1320, 2008.

[42] M.-S. Abdelouahab, N.-E. Hamri, and J. Wang, "Hopf bifurcation and chaos in fractional-order modified hybrid optical system," *Nonlinear Dynamics*, vol. 69, no. 1-2, pp. 275–284, 2012.

[43] G. De Ninno and D. Fanelli, "Controlled Hopf bifurcation of a storage-ring free-electron laser," *Physical Review Letters*, vol. 92, no. 9, Article ID 094801, 2004.

[44] C. Yuan and J. Wang, "Hopf bifurcation analysis and control of three-dimensional Prescott neuron model," *Journal of Vibroengineering*, vol. 18, no. 6, pp. 4105–4115, 2016.

[45] N. Yang, C. Xu, C. Wu, R. Jia, and C. Liu, "Dynamic behaviors and the equivalent realization of a novel fractional-order memristor-based chaotic circuit," *Complexity*, vol. 2018, Article ID 9467435, 13 pages, 2018.

[46] V. Springl, W. Jaikla, and M. Siripruchyanan, "Floating positive/negative resistance simulators employing single dual-output OTA," in *Proceedings of the 2006 International Symposium on Communications and Information Technologies*, pp. 352–355, IEEE, Bangkok, Thailand, October 2006.